Polyoxometalate Coordination Polymers Enhance Electrocatalytic Hydrogen Evolution in Trimetallic Sulfides

Shuyuan Zhang[a], Guangning Wang[a], Jie Liu[a], Qian Wang[a], Chunjing Zhang*[b,c], Haijun Pang[d], Xiaoyi Li[a], Shiming Wang[a], and Tingting Chen*[a]*

Table of contents

Section 1 Experimental Section

I. Materials characterization

All reagents are commercially purchased and used directly. The X-ray powder diffraction (XRD) spectra date was obtained by Rigaku D/max2600 X-ray diffractometer. Meanwhile, the scanning electron microscopy (SEM; S-4088, Hitachi) equipped with an energy-dispersive X-ray spectroscopy (EDXS) assisted elemental mapping and transmission electron microscopy (TEM; FEI, Tecnai TF20) was used to characterize the morphology of the material. Fourier transform infrared spectroscopy (FTIR) spectra on KBr pellets were recorded on a Nicolet AVATAR FT-IR 360 spectrophotometer in the range 500-4000 cm^{-1}. The Raman spectroscopy analysis was performed at the NanoBase Compact and The X-ray photoelectron spectroscopy (XPS) measurement was measured by a Kratos AXIS SUPRA+ with a monochromatic Al Kα source.

II. Single Crystal X-ray crystallography

Single-Crystal Structure Determination: Single-crystal X-ray diffraction data collection of the compound **1** was performed by using a Bruker Smart Apex CCD diffractometer with Mo-K a radiation (λ= 0.71073 Å) at 296 K. Multiscan absorption corrections were applied. The structure of **1** was solved by direct methods and refined on F^2 by full-matrix least-squares methods using the SHELXTL package[1]. The organic hydrogen atoms were generated geometrically. Crystallographic data and structure refinement, bond lengths and angles, and anisotropic displacement parameters have been deposited in the Cambridge Crystallographic Data Center (CCDC No.2371118 for **1**). Details of the crystallographic data and structural determination of compound **1** are listed in Table S1.

Table S1. Crystal data and structure refinement data for **1**.

Compound	**1**
Formula	$C_{20}H_{25}N_4PMo_{12}O_{41}$
M	2172.67
Crystal system	Orthorhombic
Space group	Pnma
a/Å	16.628(2)

b/Å	14.012(2)
c/Å	20.910(2)
α/deg	90
β/deg	90
γ/deg	90
V/Å³	4872(1)
Z	4
$Dcalcd$/g cm⁻³	2.962
T/K	296(2)
Refl. Unique	6211
R_{int}	0.0918
GoF on F2	1.191
R_1 / wR_2 [I >2 σ(I)][a,b]	0.0554 / 0.1245

[a]$R_1 = \sum \left\| F_o \right| - \left| F_c \right\| / \sum \left| F_o \right|$, [b]$wR_2 = \{ \sum [w(F_o^2 - F_c^2)^2] / \sum [w(F_o^2)^2] \}^{1/2}$

III. Methods of electrochemical measurement

The electrochemical test for HER of the synthetic sample was carried out by using a three-electrode system through a VMP3 (France) electrochemical workstation. A 1 cm² MoS$_2$-Ag$_2$S-NiS-NF was used as the working electrode of the experiment, at the same time, saturated calomel electrode (SCE) was used as reference electrode, and a graphite rod was employed as the counter electrode, in 1.0 M KOH at 25°C. According to the Nernst equation, combined with reversible hydrogen electrode (RHE): ERHE = ESCE + 1.07, the final potential is expressed. After the electrodes are connected, the samples are scanned for 30 cycles of Cyclic voltammetry (CV), at a voltage of -1.4 to -1 V at a sweep rate of 20 mV s⁻¹ to obtain a stable current. The Linear sweep voltammetry (LSV) was performed in the range of -1.0 to -2.0 V with a scanning rate of 5 mV s⁻¹. According to η = a + b log j (where η represents overpotential, a represents the Tafel constant, b represents the Tafel slope, and j represents current density), the tafel slope can be derived. The Electrochemical double-layer capacitance (Cdl) was calculated by CV tests at different speeds with a potential range of -0.59 to-0.40 V. In order to measure the cyclic stability of the material, CV scan 1000 laps between -1 to -1.4 V at 100 mV s⁻¹ speed. Then, the

electrochemically active surface area (ECSA) was influenced by the Cdl. The chronopotentiometry measurement (CP) was used to measure the stability of the reaction lasted for 24 hours at -10 mA cm^{-2}. Electrochemical Impedance Spectroscopy conducted at -0.25 V for HER, with frequency range is 10^5 Hz to 0.01 Hz. All data in this paper are corrected by iR-compensation.

Section 2 Supplementary electrochemical testing and characterization
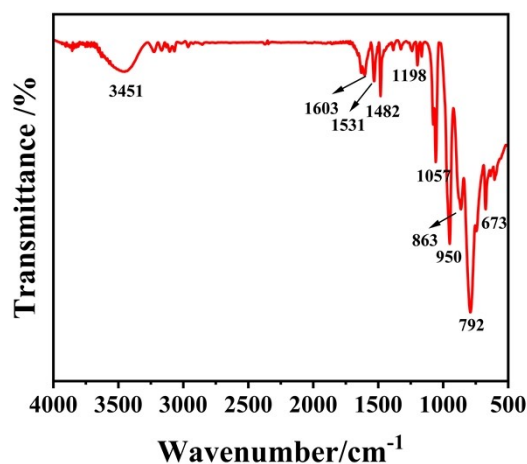
I. The FTIR spectra of compound 1

Fig. S1 FTIR spectrum of compound **1.**

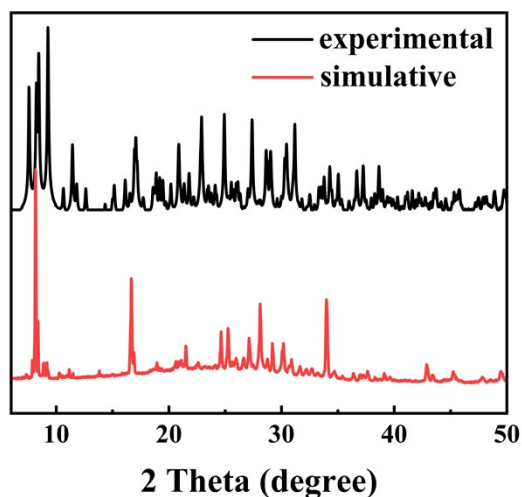### II. PXRD and single-crystal X-ray diffraction of compound 1

Fig. S2 PXRD and single-crystal X-ray diffraction of compound **1.**
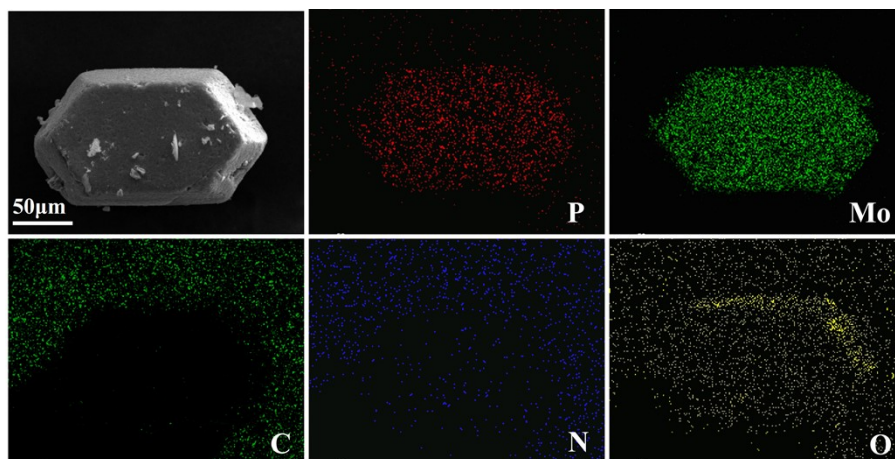
III. SEM images of the compound 1

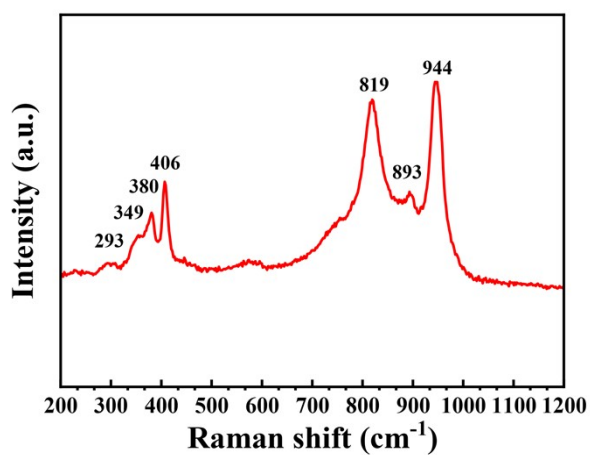**Fig. S3** SEM images of the compound **1**.

IV. Raman spectroscopy plot of MoS$_2$/Ag$_2$S/NiS@NF

Fig. S4 Raman spectroscopy plot of MoS$_2$/Ag$_2$S/NiS@NF.

V. The EDS elemental analysis of MoS$_2$/Ag$_2$S/NiS@NF

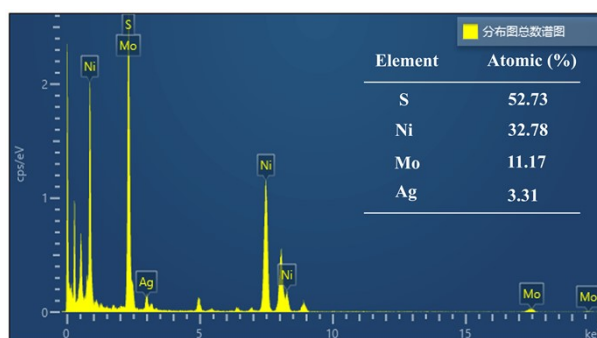| Element	Atomic (%)
S	52.73
Ni	32.78
Mo	11.17
Ag	3.31

Fig. S5 EDS elemental analysis of MoS$_2$/Ag$_2$S/NiS@NF.

VI. LSV curves and tafel slopes for different materials
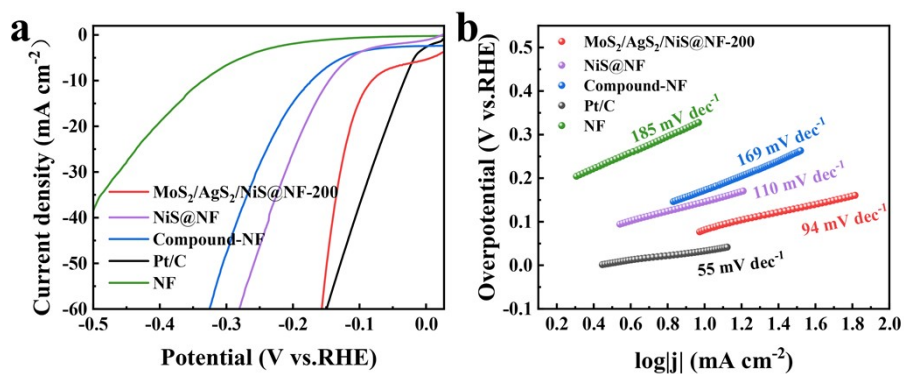
Fig. S6 (a) LSV curves of different materials. (b) corresponding HER Tafel plots.

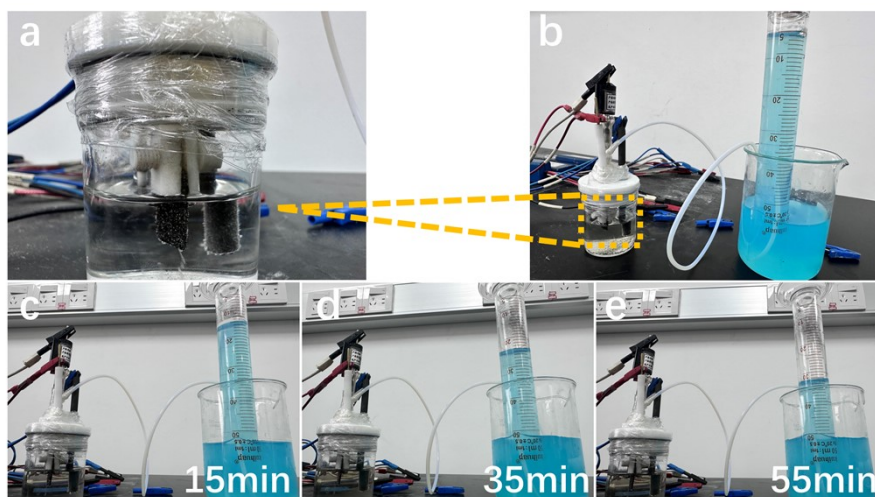## VII. Faraday efficiency testing of composites

Fig. S7 (a-b) Diagram of Faraday efficiency of total solution water determined by drainage method of Closed cell electrolyzer (c-e) The volume measurement of the gas obtained was collected at different times.

VIII. Raman spectroscopy plot before and after the reaction of MoS$_2$/Ag$_2$S/NiS@NF
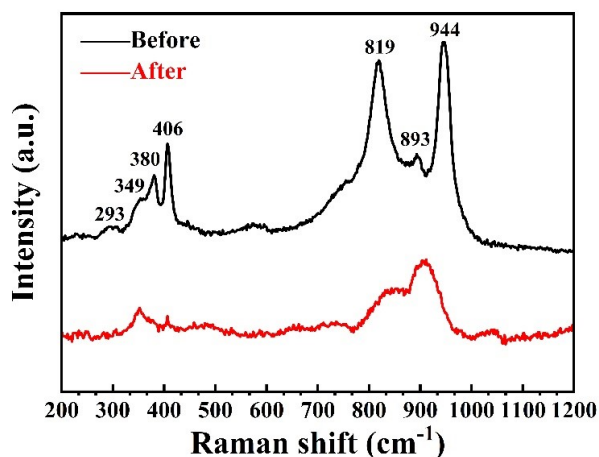
Fig. S8 Raman spectroscopy plot before and after the reaction of $MoS_2/Ag_2S/NiS@NF$.

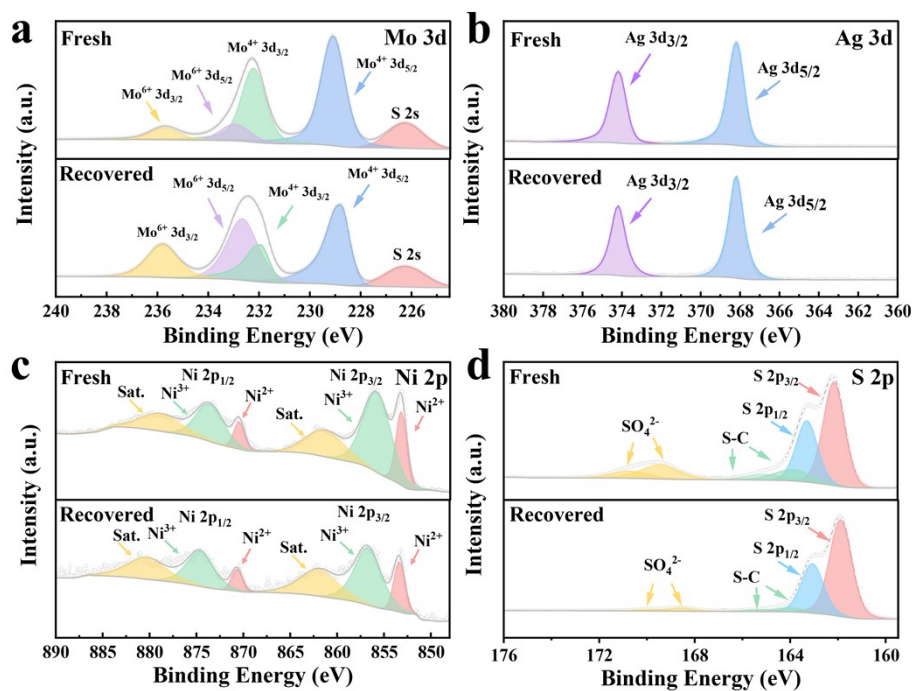## IX. XPS of the $MoS_2/Ag_2S/NiS@NF$ before and after HER reaction

Fig. S9 XPS of the $MoS_2/Ag_2S/NiS@NF$ before and after HER reaction (a) Mo 3d, (b)Ag 3d, (c) Ni 2p and (d) S 2P.

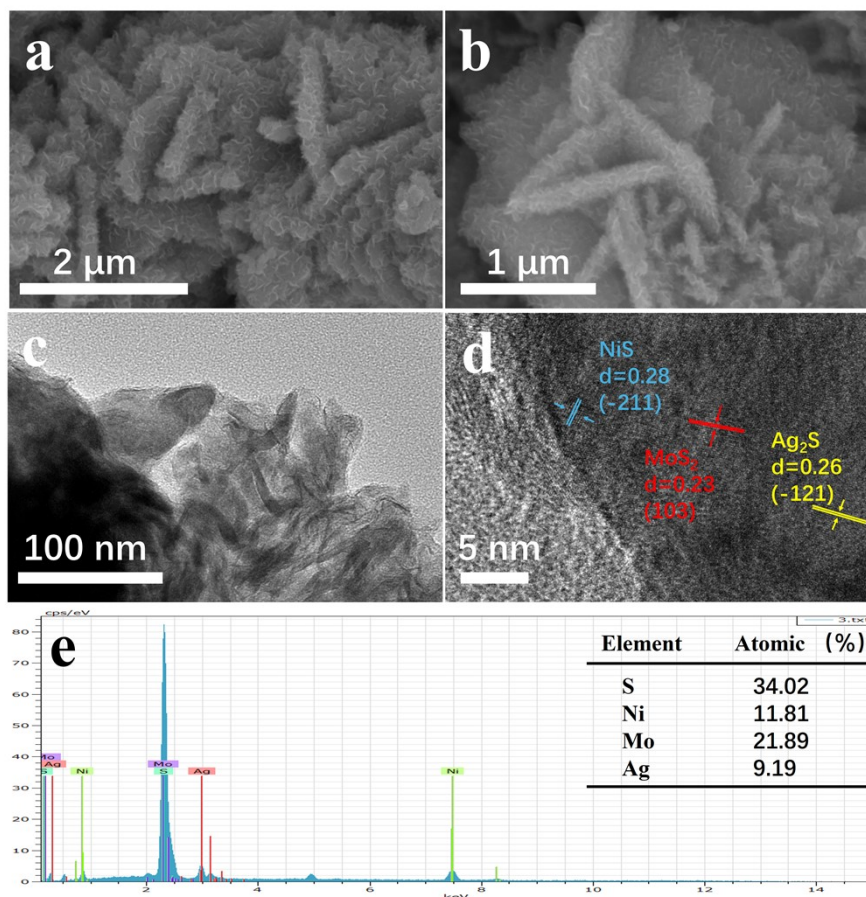## X. SEM and HRTEM of the $MoS_2/Ag_2S/NiS@NF$ after HER reaction

Fig. S10 (a-b) The SEM images of the $MoS_2/Ag_2S/NiS@NF$ after HER reaction. (c-d) The HRTEM images of the $MoS_2/Ag_2S/NiS@NF$ after HER reaction. (e) The EDS elemental analysis of $MoS_2/Ag_2S/NiS@NF$ after HER reaction.

XI. The reaction mechanism of synthetic materials as electrode materials

Electrochemical water decomposition is the decomposition of water into H_2 and O_2, which plays a key role in the development of clean energy technology. The oxygen evolution reaction (OER) on the anode produces O_2, and the hydrogen evolution reaction (HER) on the cathode produces H_2, which usually requires extremely high overpotential, which makes the selection of efficient and economical water cracking catalysts essential [2-3]. The reaction equations and principles Fig. S11. are as follows.

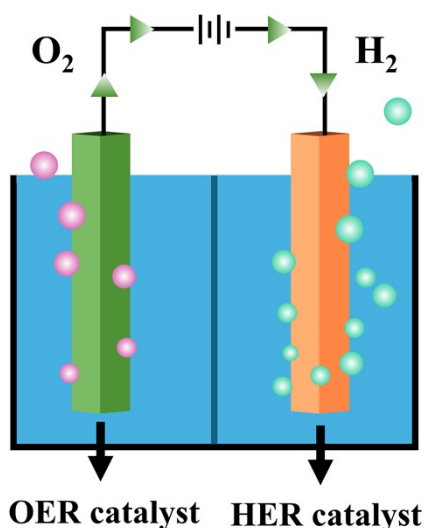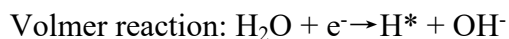$$2H_2O \rightarrow O_2 \text{ (g)} + 2H_2 \text{ (g)}$$
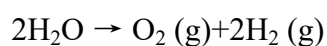
Fig. S11 A diagram shows the principle of electrolysis of water

HER is generally considered a double electron transfer process. In the alkaline medium, since there are no hydrogen protons, the hydrogen protons that are adsorbed on the surface of the catalyst are provided by water molecules. The reaction steps are as follows:

$$Volmer\ reaction: H_2O + e^- {\rightarrow} H^* + OH^-$$

$$Heyrovsky\ reaction: H^* + H^+ + e^- {\rightarrow} H_2O$$

$$Tafel\ reaction: 2H^* {\rightarrow} H_2$$

In this paper, the polyoxometalate-based coordination polymer synthesized compound **1** has low activity to decompose water under alkaline conditions and cannot provide enough hydrogen ions. Fortunately, considering that metal sulfides are widely used in the field of electrocatalytic hydrogen evolution, it just happens that there are metal ions in the synthetic materials, consequently, synthetic crystalline material is used as precursor and nickel foam as substrate to form trimetal sulfides. After vulcanization treatment, the active site of the material is greatly improved, and enough hydrogen ions can be provided to improve the efficiency of hydrogen evolution. To sum up, a new type of catalyst with good performance of electrocatalytic hydrogen evolution have been successfully synthesized.

references:

[1] G. M. Sheldrick, SHELXTL (version 6.10), Madison, WI, 2000.

[2] J. Lu, W. Zhou, L. Wang, J. Jia, Y. Ke, L. Yang, K. Zhou, X. Liu, Z. Tang, L. Liu and L. Chen, ACS Catal., 2016, **6**(2): 1045-1053.

[3] J. Tang, R. Salunkhe, J. Liu, N. Torad, M. Imura, S. Furukawa and J Am Chem. Soc., 2015, **137**(4) :1572-80.